Light Metals 2014
Edited by: John Grandfield
TMS (The Minerals, Metals & Materials Society), 2014

ALUMINUM TAILOR-WELDED BLANKS FOR HIGH VOLUME AUTOMOTIVE APPLICATIONS

Yuri Hovanski[1], Piyush Upadhyay[1], Siva Pilli[1], Blair Carlson[2], John Carsley[2], Susan Hartfield-Wunsch[2], Mark Eisenmenger[3]
[1]Pacific Northwest National Laboratory, 902 Battelle Boulevard Richland, WA
[2]General Motors,
[3]TWB Inc.

Keywords: Aluminum Tailor welded blanks, 5xxx, Friction Stir Welding, Dissimilar thickness, Design of Experiment

Abstract

Design of Experiment based approach is used to systematically investigate relationships between 8 different welding factors and resulting weld properties including strength, elongation and formability in 1.2mm-2mm thick friction stir welding of AA5182-O for TWB application. The factors that result in most significant effects are elucidated. The interactions between several key factors like plunge depth, tool tilt, pin feature and pin length on the overall weld quality is discussed. Appropriate levels of factors that lead to excellent weld properties are also identified.

Introduction

The use of tailor welded blank (TWB) technique has enabled automotive manufacturers to optimize material use in sheet metal assembly by selectively varying material thickness, alloy and/or temper type and surface coatings. Over the years developmental work in TWB technologies mostly in steels has resulted in weight and cost reduction proving the effectiveness of TWB over conventional assembly methods.[1–3] However, there is a continued push to further decrease vehicle weight and hence fuel consumption and emissions.[4] Vehicle technology office under the US department of energy has set the goal of 50% reduction in weight of passenger-vehicle body and chassis system by 2015 compared to 2002 Vehicle.[5] To this end automotive manufacturers and stakeholders have identified the use of weight saving, aluminum alloy as a viable replacement of steel in several automotive structural components.

Aluminum alloys offer several advantages over steels including high strength to weight ratio, corrosion resistance and recyclability. However aluminum TWBs come with unique challenges that need to be overcome before aluminum can be readily used as a steel substitute. In addition to being able to produce defect free welds it is of the utmost importance to have desirable post-weld formability properties for subsequent stamping processes. It is also desirable be able to produce welds at high speed to meet high volume requirements. Hence recognition and detailed development of the welding methods that fulfill all these requirements are being pursued by several researchers and stakeholders.

Several fusion welding methods have been employed to join aluminum alloys for TWB applications including gas tungsten arc welding (GTAW), laser of various types, resistance mash welding, and electron beam. [6–8] These methods produce TWBs with their own unique characteristic properties. However, all these methods employ local melting in some degree. Since aluminum has high reflectivity, low molten viscosity and inherent affinity to oxide formation, fusion welding methods increase susceptibility to porosity, hot cracking and element loss in the weld seam. Thus volumetric defects and strength reductions are difficult to avoid.

Being a solid state joining method, Friction Stir Welding (FSW) does not require melting; thus, avoids the problems faced by fusion welding. FSW utilizes frictional heating and plastic deformation enabled by a non-consumable rotating tool to produce a welded joint between abutting faces. Over the years with extensive research and development in industry and academia on weld process parameters and tool designs, friction stir welding has emerged as a viable technique to join aluminum alloys producing defect free welds with significant improvement in strength, ductility, corrosion resistance and reduced distortion.[9–12]

A critical issue in applying FSW to TWB application is finding weld process parameters including tool design and control variables that yield defect free welds with mechanical properties that withstand large multidirectional strains during stamping at a reasonably competitive speed for high volume production. Several researchers have studied formability characteristics of FSW joints. Sato et al examined the relationship between weld microstructure and formability characteristic in 2mm thick 5052-O alloy for automotive applications. They used a combination of shoulder diameters ranging from 9-15mm, rotation speeds from 2000-4000rpm and travel speeds of 0.5-2m/min. In total 7 conditions demonstrated defect free welds. The authors found that larger grain size and lower dislocation densities in the nugget lead to excellent formability characteristics in plain strain deformation.[13] Miles et al reported FSW in sheets of 5182, 5754 and 6022 (all ~2mm thick) in dissimilar combinations at different traverse and rotational speeds. [14] Successful welds between 5182 and 5754 were obtained at welding speeds of 0.24m/min and 0.4m/min and rotational speed of 1000 and 1500rpm. For both tensile and limiting dome height tests most of the welds failed at the base metal indicating a stronger nugget region. (Vickers Hardness measured were 10-15HV higher than base metal. Most of the strain during testing was concentrated in the weaker 5754 resulting in 18% elongation and Limiting Dome Height (LDH) punch stroke 27mm. Peel et al reported defect free welds between 5083-6082 and some 5083-5083 (all 3 mm thick) within the welding speed of 0.1m/min to 0.3m/min and rotational speed of 280-840rpm.[15] They found that tool rotational speed was most significant in determining the temperature regime and material mixing in the weld. The highest elongation during transverse tensile test was only 6% while the strength value was also significantly lower than the base metal. Lee et al studied the formability characteristics of FSW 5083-O and 5083-H18 made at the welding speed of 0.3m/min at 1000rpm.[16] Citing the LDH test and simulation studies the authors suggested that the orientation of the weld line with respect to the principal loading

direction during the forming process our important in determining the strain localization at failure.

There are few works, some in FSW but most in fusion welding that have investigated the strength and formability characteristics of joints made in dissimilar thickness configurations. Davies et al joined 5182-O (1mm to 2mm) using gas tungsten arc welding. They established forming limit diagram of TWB for the sheet using miniature tensile tests from welded samples. Stephens et al and Chung et al performed LDH tests and uniaxial tests to determine formability limit of FSW 5182 (1mm-2mm, 1.2mm-1.6mm respectively).[17, 18] With the change in thickness between two joining sheets, material and property discontinuity is introduced thus leading to reduced formability properties in the weld. In AA7075 for example, Buffa et al reported a ~60% decrease in the joint efficiency as the thickness ratio was changed from 1 to 1.33.[19] Raymond et al showed using simulation and experimental data that the ductility of dissimilar thickness joint reduces rapidly as the thickness ratio increases to around 1.25 and beyond.[20]

Most of the works available in the literature have studied formability properties of FSW joints in similar thickness configurations and without much emphasis on weld parameter optimization. Thus there is a dearth of information on the effects various welding control parameter have on weld formability and other mechanical properties for TWB applications.

The objective of the present study is to fill that gap and to evaluate the relationship between several welding parameters and resulting weld properties of friction stir welds in dissimilar thickness configurations. As such, we hope to establish a methodology that will be helpful in choosing certain control parameters and tool geometries that achieve optimum TWB properties for automotive applications. Weld formability, tensile strength and elongation, hardness distribution and weld quality are reported and correlated with the weld parameters and tool design.

Experimental Details

2.1 Base Metal

All the welding reported in this work was performed between 1.2mm and 2.0mm thick 5182-O sheets. The chemical composition and relevant mechanical properties of AA5182-O are shown in Table 1 and Table 2. Tensile properties in Table 2 were measured using ASTM Sub size E-8 samples (38.1mm gage length) from 1.2mm thick sheet, while the hardness data was obtained using a Vickers hardness indenter with 300gm load and 10 seconds of loading time. AA 5182-O is a non-heat treatable, solid solution strengthened Al- Mg alloy. AA5182 has been an alloy of choice for the automotive structural application owing to its excellent ductility and formability characteristics.

Table 1 Chemical composition of AA5182-O

Mg	Fe	Mn	Si	Zn	Cu	Cr	Ti
4.0-5.0	0.35	0.2-0.5	0.20	0.25	0.15	0.1	0.1

Table 2 Relevant Mechanical properties of AA5182-O

Yield Strength, MPa	Ultimate tensile Strength, MPa	Elongation at break(25.4mm gage)	Vickers hardness
130	295	23%	71

2.1 Welding Experiments

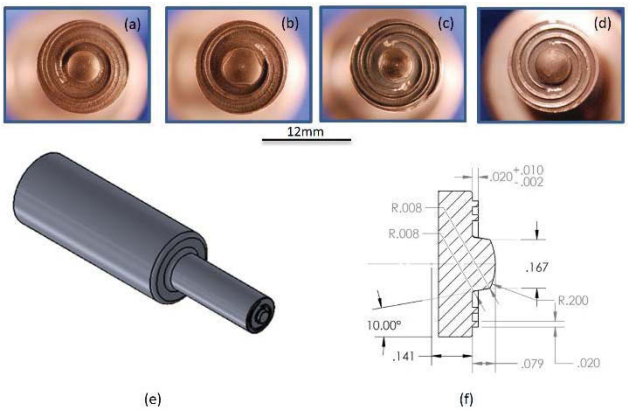

Figure 1 Top views of some representative tools used for the experiments. a) Tapered Pin, single scrolled shoulder, shoulder to pin ratio (S/P) =3 b) Pin with 3 flats, single scrolled shoulder, S/P =2.5:1 c) Pin with 3 flats, double scrolled shoulder, S/P =3 d) Threaded Pin, double scroll, S/P =3 e) Isometric view of the tool d) detail of pin and shoulder geometry of tool shown in (c). f) Schematic cross-section of a 2mm long pin with three flats, double scrolled shoulder with S/P=3

Welds were produced on high precision FSW machine located at Pacific Northwest National Laboratory. The FSW system can measure several process responses in real time including tool forces in all three directions, tool torque and position. Each weld panel being joined were 609mm long and 229 mm wide resulting in a total weld length of 550mm. The thick side was always positioned as the advancing side of the weld.

Table 3 List of 8 welding control variables and levels at which the factors were varied.

Control Variables	Levels:		
Plunge Depth	1.85mm (Shallow)	2.0mm (Deep)	
Tool Tilt	0° (Zero)	1° (One)	
Anvil Tilt	3.0° (Less)	3.82° (Tangent)	
Shoulder Dia/ Pin Dia.	2.5:1(High)	3:1(Low)	
Shoulder Scrolls	1	2	
RPM	1950	1500	1100
Pin Feature	Taper	Flats	Threads
Pin Length	1.5mm	1.75mm	2.0mm

The goal of the study was to systematically investigate the effects of various welding factors on resulting weld quality and mechanical properties. To this end 8 different welding factors: 4 pertaining to tool geometry and 4 pertaining to weld process control were varied at several levels. Factors levels or the Design Matrix was obtained using Taguchi Design of Experiment approach in Minitab™. The Taguchi method used a structured and organized dataset to define relationships between process factors and responses with a significantly reduced number of experiments compared to full factorial runs. A total of 36 runs were prescribed by Minitab™ which resulted in a total of 33 unique tool designs and different combinations of weld control variables. The 8 factors and different levels in which each was varied are shown in

tabulated format in Table 3. Plunge depth indicated the downward Z distance that the tool was commanded to move from the surface of the thicker sheet. The tool tilt, inclined towards the trailing edge defines the angle between the tool axis and normal to the work-piece surface along the weld length. In order to accommodate for the difference in sheet thickness between abutting surfaces, a steel anvil was inclined such that the thin side was raised from the horizontal plane. This anvil angle insured that the shoulder surface was flat with the slanted abutting surfaces. Two anvil angles are used, one tangent to the abutting faces, another slightly less than tangent. Three types of pin features were used including: tapered pins (10° taper), pins with flats (3 equally spaced flats 0.25mm deep) and threaded (1.5mm pitch) pins. See Fig. 1 for tool geometry and representative dimensions. All the tools had a nominal shoulder diameter of 12.7mm. All the welds were made at 3m/min with three distinct rotational velocities as shown in Table 3 Welds were made utilizing a position control scheme such that there is a fixed distance between the tool and the work piece throughout the length of the weld. The forge forces experienced by the tool for these sets of experiments ranged from 9kN- 13kN while the transverse forces on the tool ranged from 1.2-2.6kN.

Results and Discussions

Table 4 shows four different weld cases out of the total 36 runs that yielded superior strength, formability and overall weld quality. All the weld cases shown in the table have final fracture in the thin base metal for both tensile and LDH tests while the weld region remained intact. The flash level and consolidation observed visually were also excellent in all four cases shown in the table. The R_a and R_{max} values indicated corresponds to the surface roughness of the weld crown measured using a high magnification optical method. Figure 2 shows 3D surface roughness profiles for Weld #1 and #2 indicating key roughness parameters. Some variation in surface roughness is apparent between different weld parameter sets. Weld#1 produces the smoothest weld surface. It is also to be noted that the surface roughness values are independent of the extent of the flash obtained during the weld. Figure 3 shows micro hardness distribution for weld condition #1 along the weld transverse direction at three different Z depths. The weld nugget is slightly harder than the base metal (approx. 15-18HV harder). This increased hardness in FSW 5182-O has been observed in prior work by Miles et al[14] and Leito et al[21] and can be attributed to significant decrease in the grain size leading to greater pinning of dislocations and residual work hardening because of large strain during welding. It is also interesting to note that the nugget hardness is highest near the crown and decreases towards the root perhaps because of greater material flow and hence greater work hardening achieved at the crown compared to the root.

Figure 4 shows stress/strain curve for transverse weld specimen obtained from weld #1 and #2 (See Table 4 for weld parameters). The corresponding stress strain curve for the base metal (1.2mm thick) is also plotted for comparison. The ultimate tensile strength of both the welds is very close to that of the base metal. For all the six samples obtained from beginning, middle and end of the weld for each case, failure consistently occurred outside of the weld in the base metal. Ductility of both the weld specimen, however is clearly lower, reduced to ~12% from ~23% in the basemetal for nominal gage length of 1.25mm. This reduction in the effective weld ductility despite a strong defect free weld is a direct consequence of geometric discontinuity caused by thickness difference of the two adjoining sheet.[19,20] If the weld contains volumetric defects the failure will undoubtedly occur in the weld leading to very poor ductility values. However both the welds #1 and #2 are defect free. In addition, the nugget region is harder than the base metal. This leads results in strain localization in statically weakest region of the sample- the thin sheet adjacent to the weld. This localization can be illustrated by considering the strain distribution in a tensile sample right before failure. The picture on the left in Figure 4 shows a strain color map obtained from digital image correlation technique few seconds before the failure during a tensile test of sample welded using weld condition #1. Clearly the strain localization occurs adjacent to the weld reducing the effective gage length by roughly half compared to the monolithic sample test.

Table 4 Welding condition out of the tested 36 runs that yielded best combination of welding properties. R_a and R_{max} values are associated with the weld surface roughness measurements.

#	Plunge Depth	Tool Tilt	Anvil Tilt	Shoulder/Pin Ratio	Scroll	RPM	Pin Feature	Pin Length	Strength, MPa	% Elong.	LDH	R_a, Rm_{ax}
1	Deep	one	tangent	low	2	1950	flats	2	297.7	12.4	20.8	29.4, 33.7
2	Deep	one	less	low	1	1500	taper	2	297.5	11.9	20.90	36.3, 47.8
3	Shallow	zero	tangent	low	1	1500	flats	1.75	294.4	11.2	18.0	87.8, 96.3
4	Shallow	one	less	high	1	1950	taper	1.75	290.5	9.0	13.9	228.1, 197.4

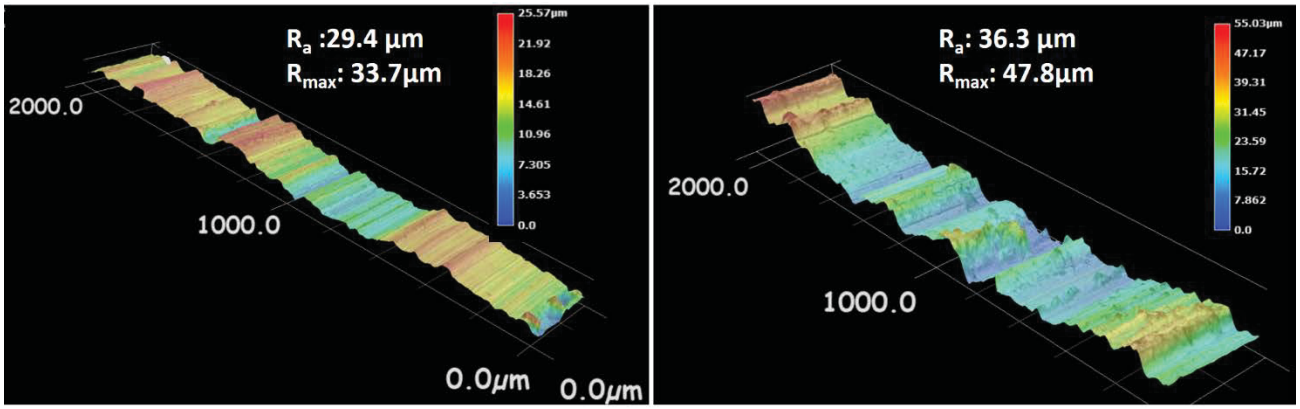

Figure 2: 3D surface profiles form weld#1 (left) and weld #2 (right) obtained from high magnification optical means.

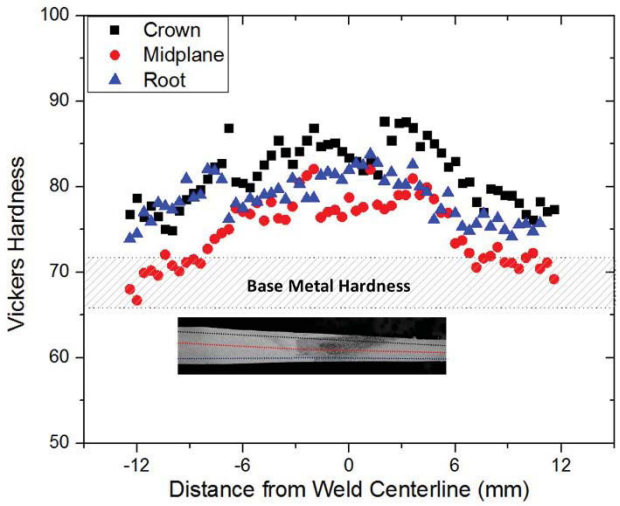

Figure 3 Micro hardness distribution along the weld crossection near the crown, in the midplane and near the root.

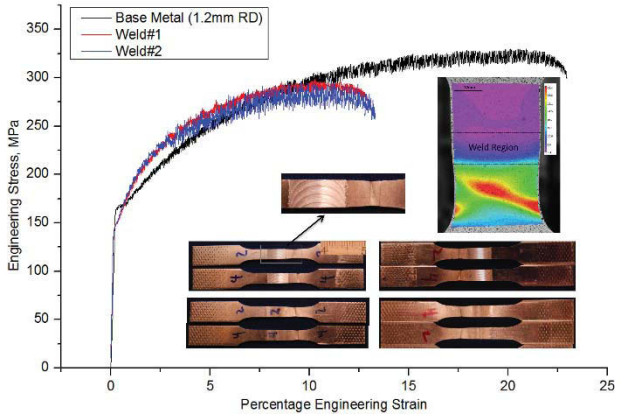

Figure 4 Stress vs. Strain curve for Weld#1 and #2. The pictures in inset shows tested samples indicating failure locations. The strain color map obtained from DIC technique is also included to illustrate strain localization.

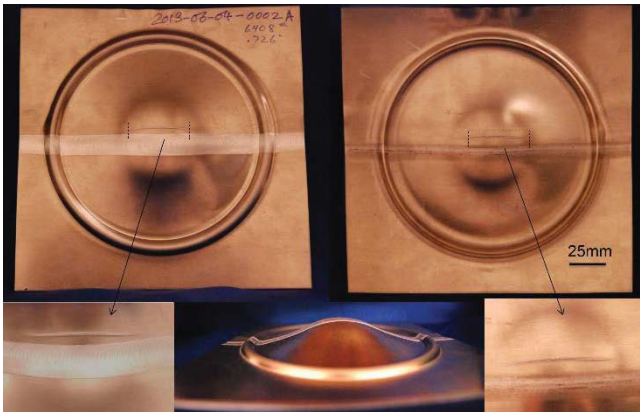

Figure 5 Limiting Dome Height tested samples corresponding to Weld#1 showing the defect location away from the weld in the thin sheet.

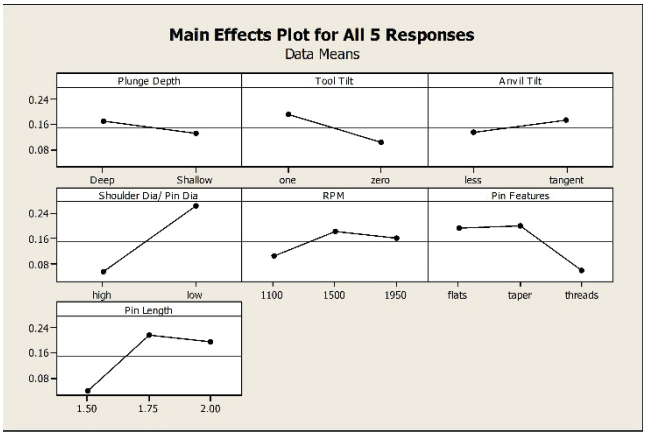

Figure 6 Main effects plots for all the 5 responses combined.

The formability characteristics of the welded samples were evaluated by performing limiting LDH tests on FSW panels. An Interlaken servo-controlled hydraulic press was used to perform the test with standard size test tool geometry using a sample size of 178mm × 178mm. Given that the welded panel consisted of sides with different thickness an appropriately size circular steel shim (0.8mm thick) was used to obtain uniform thickness around the edges. The blanks were loaded until a 5% drop in punch load was observed. The LDH was calculated simply by multiplying the punch stroke time and the punch rate (0.2mm/s). Figure 5 shows

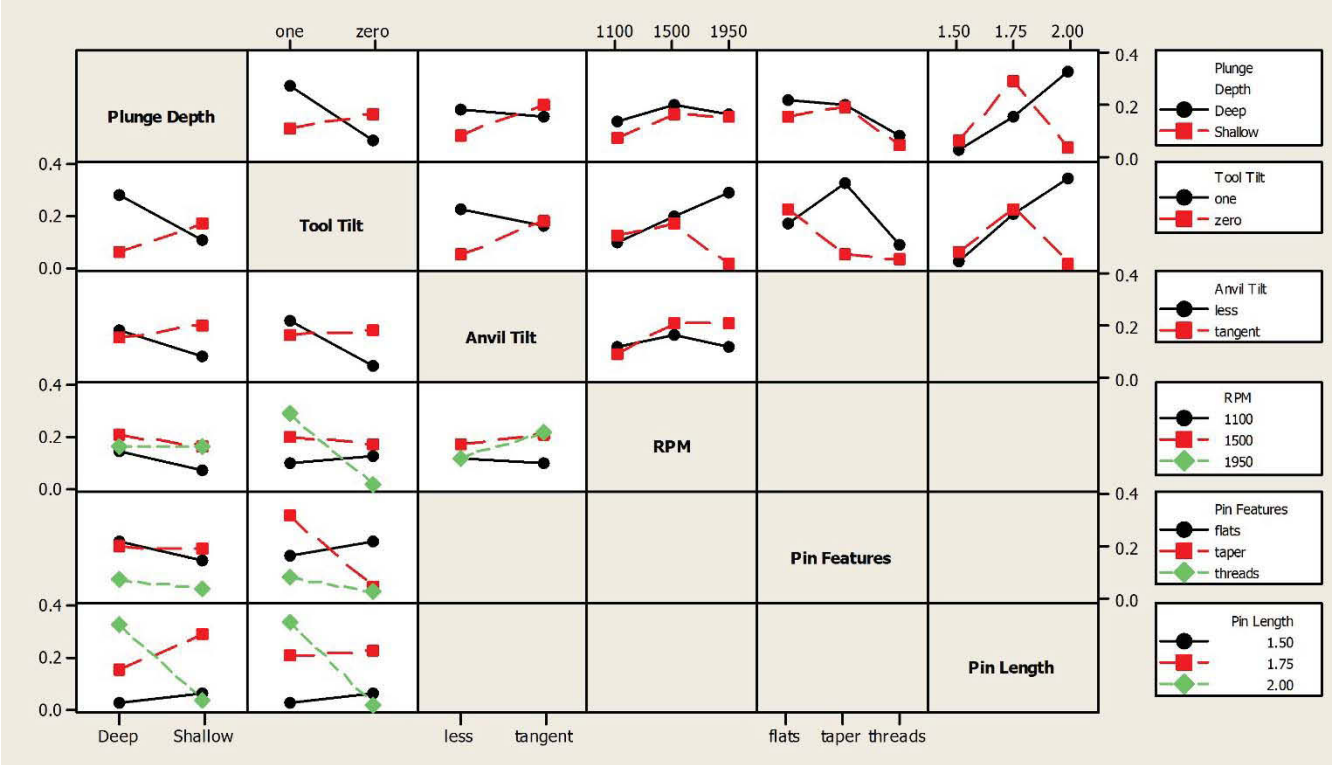

Figure 7 Interaction Plot for all the five responses combined. Note that Pin diameter is omitted from interaction plot because no significant interaction exist, however pin diameter has the largest impact among all the factors for the set of experiments reported.

the crack location on a LDH test conducted on a weld sample extracted from weld condition #1.

Five weld responses viz. ultimate tensile strength, percentage elongation at failure, LDH results, level of weld flash and level of consolidation were input into Minitab™ for analysis. For the sake of convenience in comparison, all the responses were normalized before they were input into Minitab™. Note that out of the 36 weld runs, 10 cases resulted in welds with significant defects that failed completely during the over the mandrel bend tests. Hence no further mechanical tests were carried out for those sets. Nevertheless they were included in the data analysis with "0" value for the first three responses. The main effects and possible interactions effects between different factors for each response were generated and studied both individually and in different combinations. The main effects and interactions effects of factors on all the five responses combined are presented in Figure 6 and Figure 7.

With the set of input data used, it was not possible to understand the effects of the factor "no. of shoulder scrolls" in statistically significant certainty, thus meaningful relationship was not obtained between "no. of scrolls" and other factors or the weld properties. Similarly, there were few specific pairs of factors for which relationships were not statistically certain. Hence few blocks in the interaction plot (Figure 7) are empty. This might mean that with the current number of tests input into the regression analysis were not sufficient to unravel interactions among these variables. Nevertheless several interesting relationships and interactions can be noted from the plot. The factor that causes the biggest change in the response as seen from the slope of main effects plot and p-value (0.014) from regression analysis is the Shoulder to Pin Diameter ratio. Most of the defect free welds with excellent strength and formability characteristics were obtained with tool at the low shoulder to Pin ratio (resulting in larger pin diameter = 5.0mm. Given the relatively small p-value there is no significant interaction of pin diameter with any other variable, thus the main effect plot accurately depicts the effect of pin diameter on the weld response. For this reason this factor is omitted from the interaction plot. If the main effects plot is to be believed changing the plunge depth only results in minor changes in the weld properties. Such an interpretation is convoluted by the variation in pin lengths which in combination with plunge depth can dramatically influence the final weld properties. Figure 7 shows that the longest Pin (PL=2.0mm) performs significantly better at deeper plunge compared to shallow depth (PD=1.85). The intermediate pin length however results in better response at shallow depth than deeper one. This can also be observed from the dataset shown in Table 4. Weld #1 and #2 at deep plunge depth with PL=2mm while Weld#3 and #4 at shallow depth with PL=1.75. For 1.75mm long pin, a Pin Depth of 2.0mm implies excessive shoulder engagement leading to overheated crown and less than ideal material flow. The same pin depth for a 2.0mm long pin however appropriately seats the shoulder and leads to greater mixing at the root as well. Lastly the shortest pin (PL= 1.5mm) yields poor response for both the plunge depths and hence is not desirable. A similar relationship exists between the factors pin length and tool tilt, as with a longer pin it is critical to have one degree tool tilt for acceptable weld properties. For the intermediate and short pins the tool tilt does not show much difference in response. Overall, pin lengths of 1.75mm and 2.00mm yield desirable weld properties under certain combinations of other factors as discussed above, whereas the shortest pin performs poorly under all conditions studied herein.

With regards to the tool rotation speed it is clear from the main effects and interaction effects plots that 1100rpm yields poor responses in all the combinations. 1500 and 1950rpm on the other hand performs significantly better at certain combinations of other factors. While changing plunge depth and anvil tilt causes marginal difference in weld performance for both 1500 and 1950rpm, the tool tilt of 0° causes a significant drop in weld quality for 1950rpm as seen in the interaction plot. This is perhaps indicative of the importance of greater forging action facilitate by the tool tilt at the trailing edge of the tool at higher temperature and hence softer matrix material.

Conclusion

A Taguchi based design of experiment approach was used to understand the relationship between 8 different welding factors and five key weld property responses in dissimilar thickness 5182-O for TWB application. Several relationship and interaction among different factors were revealed and a set of optimized weld control parameters was established.

References

[1] Merklein M., Johannes M., Lechner M., and Kuppert A., "A Review on Tailored Blanks - Production, Applications and Evaluation," Journal of Materials Processing Technology.

[2] Pallett R., and Lark R., 2001, "The use of tailored blanks in the manufacture of construction components," Journal of Materials Processing Technology, **117**(1–2), pp. 249–254.

[3] Brad L Kinsey, 2011, "Tailor Welded Blanks For Automotive Industry," Tailor welded blanks for advanced manufacturing, Woodhead Pub., Cambridge; Philadelphia, pp. 164–180.

[4] "President Announces New Fuel Economy Standards | The White House" [Online]. Available: http://www.whitehouse.gov/blog/2011/07/29/president-obama-announces-new-fuel-economy-standards.

[5] 2012 DOE Vehicle Technologies Office Annual Merit Review- Entire Document.

[6] Assunção E., Quintino L., and Miranda R., 2010, "Comparative study of laser welding in tailor blanks for the automotive industry," Int J Adv Manuf Technol, **49**(1-4), pp. 123–131.

[7] Davies R. W., Oliver H. E., Smith M. T., and M.s G. J. G., 1999, "Characterizing Al tailor-welded blanks for automotive applications," JOM, **51**(11), pp. 46–50.

[8] Shakeri H. R., Buste A., Worswick M. J., Clarke J. A., Feng F., Jain M., and Finn M., 2002, "Study of damage initiation and fracture in aluminum tailor welded blanks made via different welding techniques," Journal of Light Metals, **2**(2), pp. 95–110.

[9] Mishra R. S., and Ma Z. Y., 2005, "Friction stir welding and processing," Materials Science and Engineering: R: Reports, **50**(1–2), pp. 1–78.

[10] Threadgill P. L., Leonard A. J., Shercliff H. R., and Withers P. J., 2009, "Friction stir welding of aluminium alloys," International Materials Reviews, **54**(2), pp. 49–93.

[11] Nandan R., DebRoy T., and Bhadeshia H. K. D. H., 2008, "Recent advances in friction-stir welding - Process, weldment structure and properties," Progress in Materials Science, **53**(6), pp. 980–1023.

[12] Mishra R. S., 2008, "Preface to the Viewpoint Set on friction stir processing," Scripta Materialia, **58**(5), pp. 325–326.

[13] Sato Y. S., Sugiura Y., Shoji Y., Park S. H. C., Kokawa H., and Ikeda K., 2004, "Post-weld formability of friction stir welded Al alloy 5052," Materials Science and Engineering: A, **369**(1–2), pp. 138–143.

[14] Miles M. P., Nelson T. W., and Melton D. W., 2005, "Formability of friction-stir-welded dissimilar-aluminum-alloy sheets," Metall and Mat Trans A, **36**(12), pp. 3335–3342.

[15] Peel M., Steuwer A., Withers P., Dickerson T., Shi Q., and Shercliff H., 2006, "Dissimilar friction stir welds in AA5083-AA6082. Part I: Process parameter effects on thermal history and weld properties," Metallurgical and Materials Transactions A, **37**(7), pp. 2183–2193.

[16] Lee W., Chung K.-H., Kim D., Kim J., Kim C., Okamoto K., Wagoner R. H., and Chung K., 2009, "Experimental and numerical study on formability of friction stir welded TWB sheets based on hemispherical dome stretch tests," International Journal of Plasticity, **25**(9), pp. 1626–1654.

[17] Chung K., Lee W., Kim D., Kim J., Chung K.-H., Kim C., Okamoto K., and Wagoner R. H., 2010, "Macro-performance evaluation of friction stir welded automotive tailor-welded blank sheets: Part I – Material properties," International Journal of Solids and Structures, **47**(7–8), pp. 1048–1062.

[18] E V Stephens, G. J. Grant, M. T. Smith, and R. W. Davies, 2010, Forming Limits of Weld Metal in Aluminum Alloys and advaced high strength steels, Pacific Northwest National Laboratory.

[19] Fratini L., Buffa G., and Shivpuri R., 2007, "Improving friction stir welding of blanks of different thicknesses," Materials Science and Engineering: A, **459**(1–2), pp. 209–215.

[20] Raymond S. D., Wild P. M., and Bayley C. J., 2004, "On modeling of the weld line in finite element analyses of tailor-welded blank forming operations," Journal of Materials Processing Technology, **147**(1), pp. 28–37.

[21] Leitão C., Emílio B., Chaparro B. M., and Rodrigues D. M., 2009, "Formability of similar and dissimilar friction stir welded AA 5182-H111 and AA 6016-T4 tailored blanks," Materials & Design, **30**(8), pp. 3235–3242.